


NANO EXPRESS

Open Access



Core-Shell Fiber-Based 2D Woven Triboelectric Nanogenerator for Effective Motion Energy Harvesting

Jinmei Liu^{1,2†}, Long Gu^{2†}, Nuanyang Cui², Suo Bai¹, Shuhai Liu², Qi Xu², Yong Qin^{1*} , Rusen Yang^{2*} and Feng Zhou³

Abstract

Personal electronic devices have a general development trend of miniaturization, functionality, and wearability. Their wireless, sustainable, and independent operation is critically important, which requests new power technologies that can harvest the ambient environmental energy. Here, we report a new kind of 2D woven wearable triboelectric nanogenerator (2DW-WTNG) composed of core-shell fibers via the twisting process and weaving process in the textile manufacture. The 2DW-WTNG can convert the body motion energy into electricity with an output current of 575 nA and an output voltage of 6.35 V. At an external load of 50 MΩ, it generated a maximum power density of 2.33 mW/m². Electricity can be produced from the 2DW-WTNG driven in arbitrary in-plane directions. A tiny displacement of 0.4 mm can drive the 2DW-WTNG, which verified its capability to harvest energy from small human movement. The robust 2DW-WTNG can work continuously for 12 h without obvious performance degradation.

Keywords: Wearable power source, Triboelectric nanogenerator, Energy harvesting, Mechanical durability, Power fabric

Introduction

With the fast development of the electronic technology, various portable, wearable, and even implantable personal electronic devices have been invented to make our daily life better [1–11]. Nevertheless, due to the inherent limitations of traditional batteries, such as limited capacity, short lifetime, maintenance difficulty, and environmental hazards [12–14], the increased production and wide application of personal electronic devices make pressing demands for new power supply [15–19]. It is urgently needed to develop new power sources that enable electronic devices working sustainably and timely. Body motion energy from human daily activities widely exists no matter what you do and where you are [20]. If such mechanical energy can be effectively harvested and converted into electricity, it may power personal electronic devices whenever and wherever needed.

As a new type of power-generating device to convert mechanical energy into electricity [21–24], triboelectric nanogenerators are based on the coupling of the contact electrification effect and the electrostatic induction [25–30]. They have been successfully demonstrated as sustainable power sources for portable electronics, sensors, environmental monitors, and so forth [31–44]. Among them, wearable triboelectric nanogenerator (WTNG) has been designed to convert the body motion energy from human activities into electricity [45–47]. The current WTNGs can be divided into two categories by whether a substrate is used. Most WTNGs belong to the first category and have their electrode and frictional layer coated on a flexible substrate, such as a textile fiber or a piece of fabric [48–53]. They possess good softness, flexibility, and light-weight. Nevertheless, the adhesion between the loaded electrode and the substrates is poor, which greatly reduces their durability and usability, and further makes these WTNGs unavailable for long-term usage. The second category of WTNG does not rely on extra substrate, and their building materials are directly used as the frictional layers with electrodes.

* Correspondence: qinyong@zu.edu.cn; rsyang@xidian.edu.cn

[†]Jinmei Liu and Long Gu contributed equally to this work.

¹Institute of Nanoscience and Nanotechnology, Lanzhou University, Lanzhou 730000, China

²School of Advanced Materials and Nanotechnology, Xidian University, Xi'an 710071, China

Full list of author information is available at the end of the article

A WTNG based on nylon cloth and polyester cloth skillfully avoided the adhesion issue from the substrate [54]. Later, a kind of WTNG with stainless-steel conductive thread as the electrode and silicon rubber and PDMS as the frictional layer materials were developed [55–57]. However, these WTNGs either do not have long-term robustness or have a quite complicated fabrication process which can be used in large scale fabrication.

In this work, we fabricated a new kind of 2D woven wearable triboelectric nanogenerator (2DW-WTNG) with merits of robustness and continuous production process which is well suited for large scale production. A 2DW-WTNG with a size of $1.5 \times 1.5 \text{ cm}^2$ generated an output voltage and output current of 6.35 V and 575 nA, respectively. Connected to an external load of 50 M Ω , it generates a maximum power density of 2.33 mW/m². After connected with a rectifying bridge, the 2DW-WTNG instantaneously powered a commercial light-emitting diode (LED) without any energy storage process. It was also used to charge a 0.47 mF capacitor from 0 V to 1.84 V in 1 min. Furthermore, it showed good sensitivity to external motions down to a displacement of 0.4 mm, good adaptability to work along arbitrary in-plane directions and in different working modes, and good robustness to work continuously for 12 h without degradation.

Methods

Fabrication of the Nylon/Copper Core-Shell Composite Conductive Fiber and Polyester/Steel Core-Shell Composite Conductive Fiber

The source materials for the nylon/copper composite fiber are daily sewing nylon thread (110 μm in diameter) and the enameled copper wire (60 μm in diameter). The source materials for the polyester/steel composite fiber are daily sewing polyester thread (200 μm in diameter) and the steel wire (60 μm in diameter). Two kinds of polymer/metal composite fibers were prepared using a homemade rotating support as shown in Fig. 1. For the preparation of the nylon/copper composite fiber, the enameled copper wire was first fastened at the middle of the rotating support and then two nylon threads were fixed at two ends of the rotating support. Next, the top of these three wires was held together and hung up. Finally, starting from the rotating support, nylon threads were twined and wrapped around the middle copper wire, and the nylon/copper composite fiber with core-shell structure (380 μm in diameter) was formed. The preparation for the polyester/steel composite fiber was similar to that of the nylon/copper composite fiber, in which the enameled copper wire was replaced with the steel wire and the nylon thread was replaced with the polyester thread. The core-shell structure was achieved

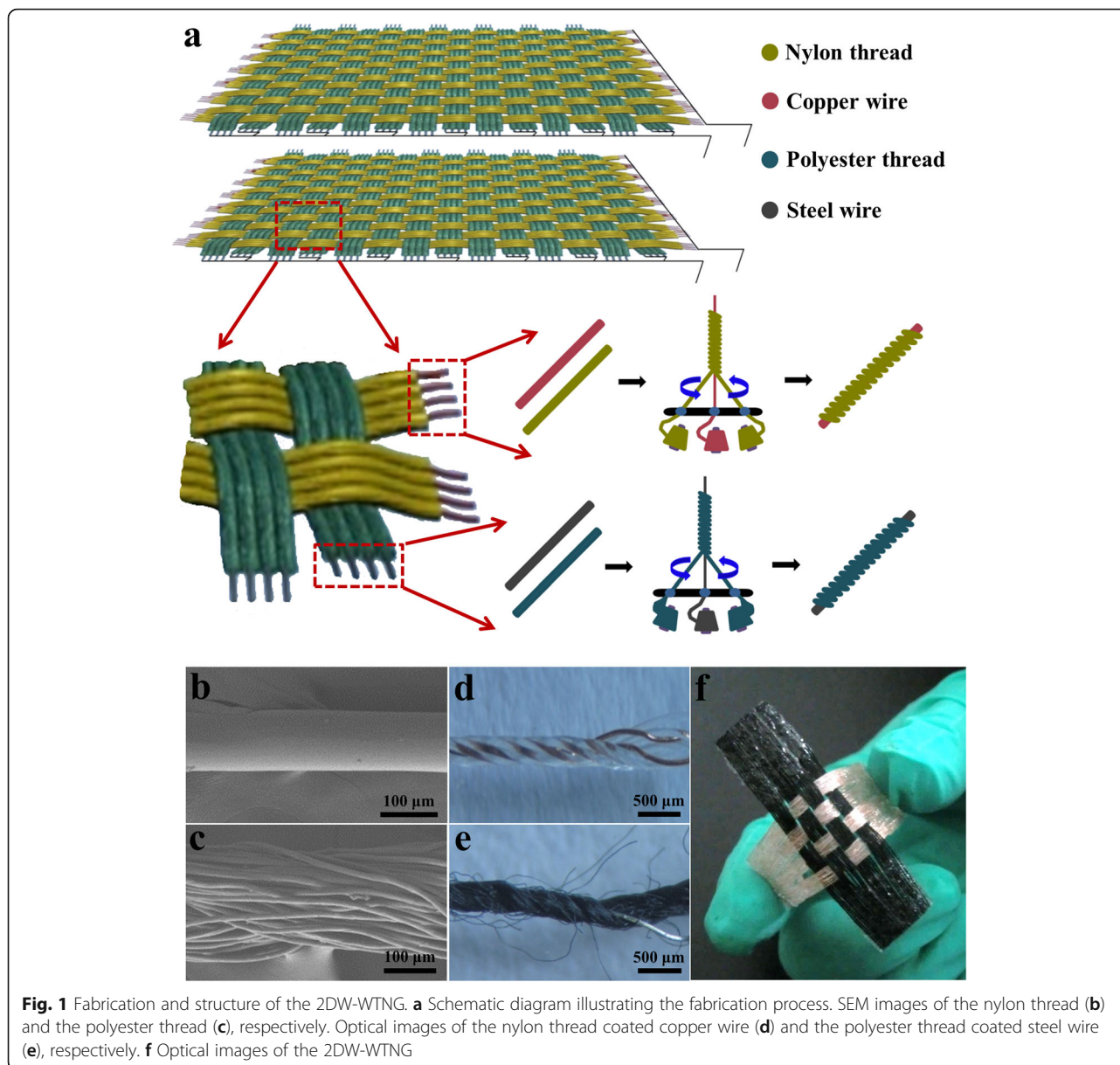
with a steel wire tightly coated with polyester thread (385 μm in diameter). Here, different metal wires were chosen to balance the stability and output performance of the 2D-WTNG. Compared with the steel, the copper wire was covered with a thin insulating layer, which was used to avoid the short circuit during the 2D-WTNG's working process. If the steel was selected to be the core electrode for both fibers, friction and abrasion might happen after a long time working, in which short circuit may occur between the positive electrode and the negative electrode. This will decrease the 2D-WTNG's stability. If the copper was selected to be the core electrode for both fibers, the electrostatic induction effect would be weakened by the insulating layer on the surface of the copper wire, which will reduce the 2D-WTNG's performance. This preparation process for the polymer/metal composite fiber imitates the model of the twist two, which is a simple tool in hand twisting thread. Using this method, the polymer/metal composite fiber can be put into mass production using a twisting machine in the factory.

Fabrication of the 2DW-WTNG

The prepared nylon/copper composite conductive fiber and polyester/steel composite conductive fiber were integrated into fabric by the general knitting technique. Nine nylon/copper composite fibers were put together side by side as a group, and nine polyester/steel composite fibers were put together side by side as a group. Two groups of nylon/copper composite fibers and two groups of polyester/steel composite fibers were knitted into the WTNG with 2D woven structure. The upper and lower parts of 2DW-WTNG have a size of 15 mm \times 15 mm (composed of 36 composite fibers) and 38 mm \times 38 mm (composed of 90 composite fibers), respectively. Their grating width was about 7 mm as shown in Fig. 1. Here, the grating width is determined by the diameter of the composite fiber and the number of the composite fiber used in one group; thus, the grating width can be conveniently adjusted by increasing or decreasing the composite fiber number in one group. This woven process can be done on loom in the factory when needing massive production.

Measurements of the 2DW-WTNG

The 2DW-WTNG with an effective size of 15 mm \times 15 mm and a grating width of 7 mm was tested by periodically moving back and forth. In the measurements, the lower 2DW-WTNG was fixed on a mechanical stage that was tightly mounted on the experimental table, and the upper 2DW-WTNG was put on top of the lower 2DW-WTNG and connected with a linear motor. Driven by the linear motor with controlled sliding displacement and velocity, the upper 2DW-WTNG makes a reciprocating linear motion in the range of the



lower one at a direction parallel to the surface of the device, which keeps the effective contact area unchanged all the time.

Results and Discussion

By using the twisting technology in the textile manufacture, a core-shell structural composite fiber was fabricated with metal wire as central electrode and sewing threads as outer frictional layers. The 2DW-WTNG was further fabricated by weaving two kinds of core-shell structured composite fibers through an orthotropic weaving process. Figure 1a shows the structural illustration of the 2DW-WTNG with two same parts. In each part of the 2DW-WTNG, nylon/copper composite fibers arranged in one direction were collected as one

electrode, and polyester/steel composite fibers arranged in the other direction were collected as the other electrode. Two kinds of composite fibers were prepared using a homemade rotating setup working like a twisting machine in factory. Scanning electron microscope (SEM) images shown in Figs. 1a and c reveal the surface appearance of the initial nylon thread with a diameter of 110 μm and polyester thread with a diameter of 200 μm , respectively. Figures 1d and e are the optical images of the prepared nylon/copper composite fiber and polyester/steel composite fiber, respectively, from which the core-shell structure can be observed distinctly. Figure 1f exhibits an optical image of the final 2DW-WTNG made of four groups of nylon/copper composite fibers and four groups of polyester/steel composite fibers. With the

woven structure in length and breadth, it resembles a piece of common cloth, and the detailed fabrication process is illustrated in the “Methods” section.

The power generation performance of the 2DW-WTNG is studied. As shown in Fig. 2a, the upper part and the lower part of the 2DW-WTNG were fixed face to face, and the upper part can slide rightward and leftward against the lower part. Once relative sliding occurred between the upper part and the lower part, the contact surfaces rubbed with each other. Since polyester is more triboelectrically negative than nylon according to the triboelectric series, electrons are injected from nylon into polyester, producing positive triboelectric charges on the nylon surface and negative charges on the polyester surface. When the upper part slid rightward and the contact surface slid into a misaligned position as shown in stage I, net electric field arose as a result of uncompensated triboelectric charges in the misaligned regions, driving free electrons from the

electrode in polyester moving to the electrode in nylon until the electric field was screened by the induced charges on electrodes. When the upper part continued sliding rightward, the contact surface came into an aligned position and the triboelectric charges of opposite signs were completely balanced, leading to a back flow of the induced free electrons (stage II). As the rightward sliding went on, the contact surface was brought back towards the misaligned position, and free electrons were driven from the electrode in polyester to the electrode in nylon as shown in stage III. Consequently, a cycle of the electricity generation process for the 2DW-WTNG was completed. Benefited from the grating design with inter-phase structure between nylon/copper composite fiber and polyester/steel composite fiber, charge alternately transferred between two electrodes during this process. Experimentally, the initial contact situation depends on how the upper part and lower part are placed. However, it will not influence the output of the 2DW-WTNG.

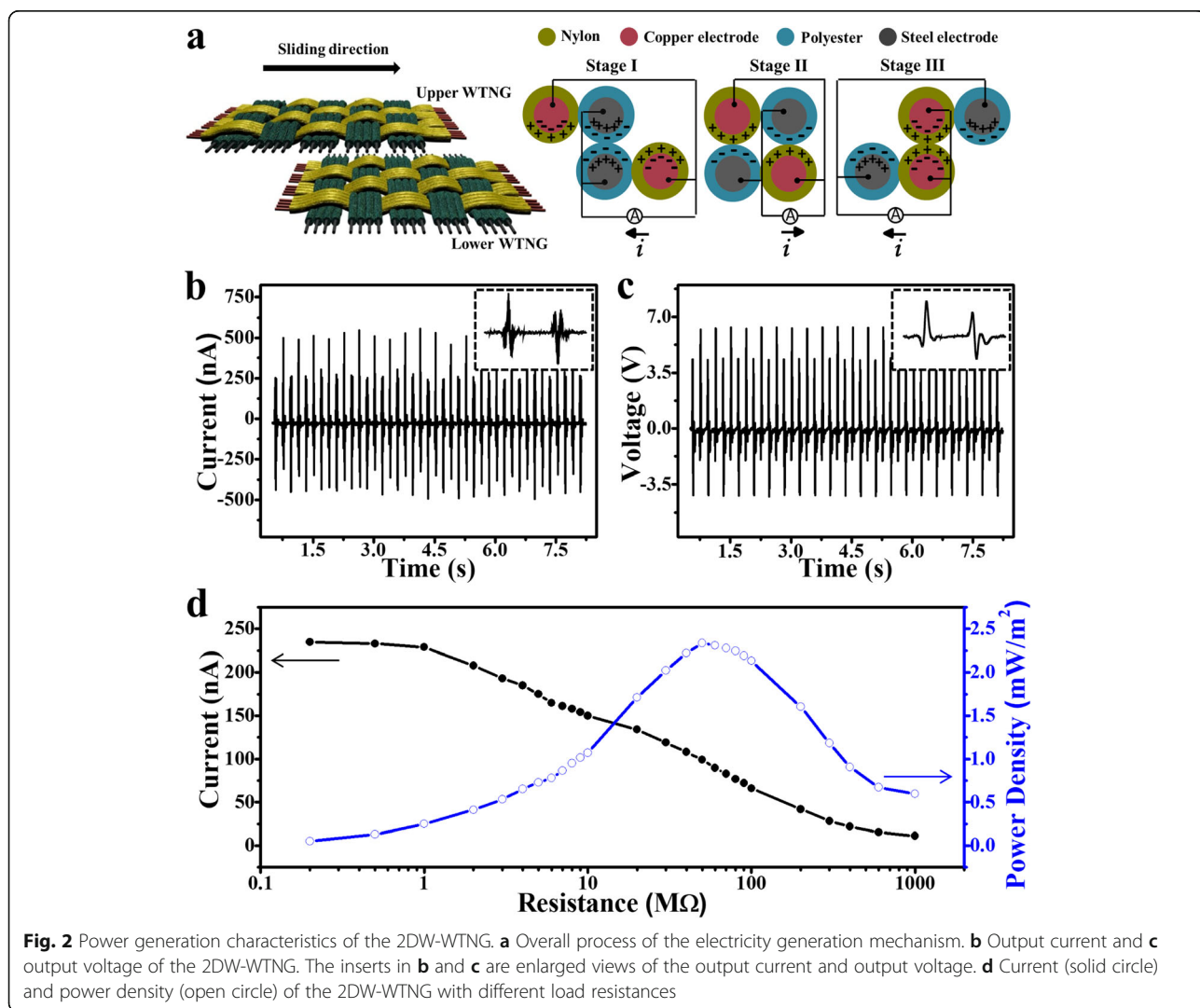


Fig. 2 Power generation characteristics of the 2DW-WTNG. **a** Overall process of the electricity generation mechanism. **b** Output current and **c** output voltage of the 2DW-WTNG. The inserts in **b** and **c** are enlarged views of the output current and output voltage. **d** Current (solid circle) and power density (open circle) of the 2DW-WTNG with different load resistances

Owing to the same grating structure, the initial contact situation makes no difference in the output peak value but changes the direction of the output peak. If the initial contact situation is positive to positive, the contact situation will first get into positive to negative and then into positive to positive with a positive output peak followed by a negative output peak. In contrast, if the initial contact situation is positive to negative, the contact situation will first get into positive to positive and then into positive to negative with a negative output peak followed by a positive output peak.

A 2DW-WTNG with a size of 15 mm × 15 mm and the grating width of 7 mm was tested by periodically moving back and forth. The detailed measurement method is illustrated in the “Methods” section. With a sliding displacement of 8 mm and a sliding speed of 0.15 m/s, the 2DW-WTNG produced a continuous alternating current (AC) output at a maximum amplitude of 575 nA at a constant frequency of 2.7 Hz (Fig. 2b). The output voltage reached 6.3 V at the same frequency as the output current (Fig. 2c). The enlarged view of the output current and output voltage in one working cycle are inserted in Figs. 2b and c, respectively. In one working cycle, there are two wave packets, one representing the one-way sliding rightward and the other representing the one-way sliding leftward. And there are two positive pulses and two negative pulses in each wave packet. This result is in accordance with the structure of device containing four groups of nylon/copper composite fibers and four groups of polyester/steel composite fibers as shown in Fig. 1f, which further verifies that the output in sliding mode is closely connected with the grating width and grating number in the device.

As a power source in practical, the 2DW-WTNG needs to be connected with external loads. Resistors were used to investigate the reliance of the output electric power on the external load. Figure 2d shows the instantaneous current and the instantaneous output power density versus the external load resistance. The instantaneous output power density was calculated as the ratio of the instantaneous output power (I^2R) and the area of the device. It was found that the instantaneous current dropped with the increase of load resistance owing to the ohmic loss. The instantaneous output power density increased at low resistances and reached a maximum value of 2.33 mW/m² at the load resistance of 50 MΩ, and then decreased at higher resistance. This result indicates the potential of the 2DW-WTNG to be a power supply for some personal electronic devices, especially for those with a load resistance about dozens of megohm.

The output performance of the 2DW-WTNG in sliding driven mode greatly relies on the separation rate of

triboelectric charge. To study this deeply, the output performance of the 2DW-WTNG with a size of 15 mm × 15 mm and a grating width of 7 mm was characterized by periodically moving at different relative sliding speeds with a given sliding displacement of 8 mm. Figures 3a and b show the output current and output voltage of the 2DW-WTNG at an average sliding speed of 0.025 m/s, 0.050 m/s, 0.075 m/s, 0.100 m/s, and 0.125 m/s, respectively. In the current curve and voltage curve, there is a full output peak in 320 ms in one-way moving and another output peak in 320 ms moving in the reverse direction at a sliding speed of 0.025 m/s. Within the same working time, an increase of the speed caused the increase of the output peak's number from one at 0.025 m/s to five at 0.125 m/s. It was because a greater sliding speed shortened the time needed for one working cycle and further increased the number of the working cycles in the same working time. The current peak value was increased from 101 nA at 0.025 m/s to 415 nA at 0.125 m/s, which implied that an increase of the sliding speed could effectively increase the separation speed of the triboelectric charge and lead to a large output peak value. The voltage peak value was increased from 3.6 V at 0.025 m/s to 6.6 V at 0.125 m/s, which was resulted from the measuring electric circuit. The input resistances of the voltage measurement circuit and the 2DW-WTNG formed a RC electric circuit, and the leakage current on the 2DW-WTNG was reduced when increasing the sliding speed, resulting in continuous enhancement of the output voltage peak value. These results clearly demonstrate that the output peak value was closely related to the sliding speed. Apart from the sliding speed, sliding displacement is another factor which largely influenced the output performance of the 2DW-WTNG. Considering that most of the mechanical energy in human body motion is from movements of small amplitude, it is thus necessary to harvest the weak mechanical energy. To explore this aspect, the 2DW-WTNG was tested by working at a sliding displacement of 0.4 mm, 0.8 mm, 1.2 mm, 1.6 mm, and 2.0 mm with a fixed sliding speed of 0.1 m/s. The output current and voltage are shown in Figs. 3c and d. Its output peak value increased with the sliding displacement. At the shortest displacement of 0.4 mm, the output peak value reached 2.3 nA and 0.05 V, respectively, exhibiting its ability of scavenging mechanical energy from small motion. According to the working mechanism of the 2DW-WTNG in the horizontal-sliding mode, there was an alternating charge transfer when sliding over one grating. Thus, it is promising to further improve the output of the 2DW-WTNG under sliding mode by narrowing the width or diameter of the woven belts or woven fibers into smaller scale.

Considering the complexity of human activities, the body motion energy may come from different directions.

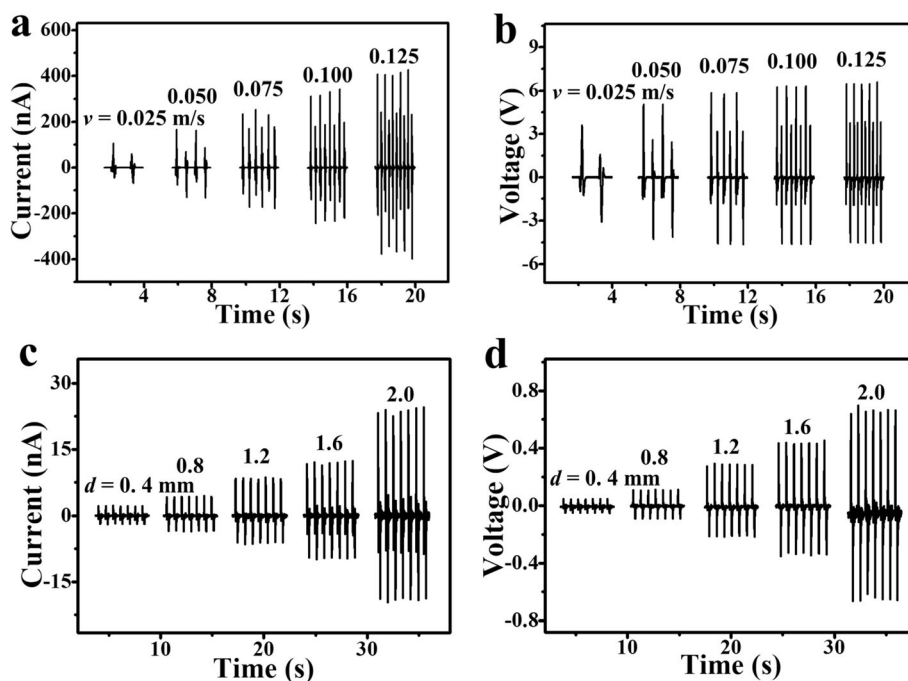
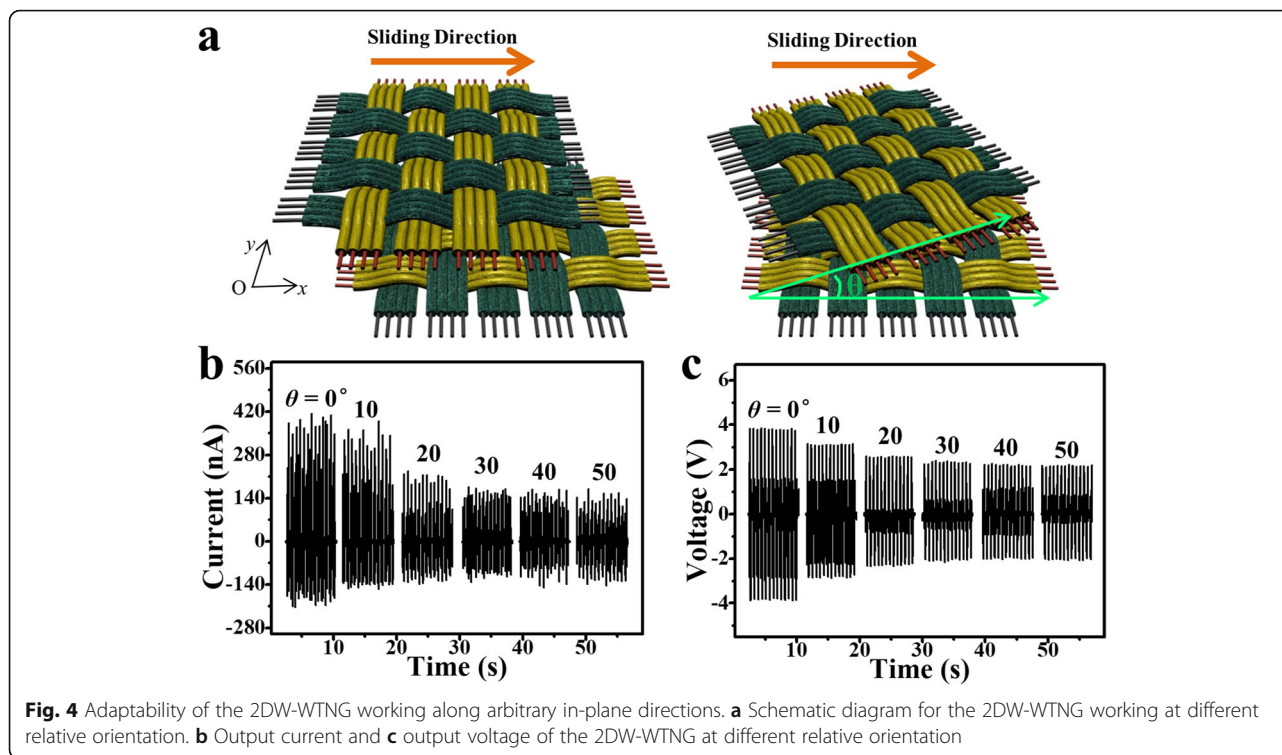


Fig. 3 Power generation performance of the 2DW-WTNG under different relative sliding speeds and relative sliding displacements. **a** Output current and **b** output voltage of the 2DW-WTNG varied with the sliding speeds of 0.025 m/s, 0.050 m/s, 0.075 m/s, 0.100 m/s, and 0.125 m/s at a given sliding displacement of 8 mm. **c** Output current and **d** output voltage of the 2DW-WTNG varied with the sliding displacements of 0.4 mm, 0.8 mm, 1.2 mm, 1.6 mm, and 2.0 mm at a given sliding speed of 0.100 m/s

Therefore, a qualified WTNG should be able to harvest energy from body movements in different directions. In other words, a WTNG working in the planar-sliding mode is expected to work along arbitrary sliding directions. As shown in Fig. 4a, two parts of the 2DW-WTNG were placed face to face and the upper part could slide over the lower part along the X -axis. Keeping the moving direction, rotating the upper part resulted in an angle (θ) between the sliding direction and one side of the upper part. Here, the θ represented essentially the relative working orientation between the upper part and the lower part of the 2DW-WTNG, which required the 2DW-WTNG to be able to work at different relative working orientations. To elucidate this, the 2DW-WTNG was tested at a set of θ values (0° , 10° , 20° , 30° , 40° , and 50°) driven by the linear motor at a sliding speed of 0.10 m/s and a sliding displacement of 10 mm. Its output current and output voltage at different θ are shown in Figs. 4b and c. The device generated an output current of 134.45 nA and an output voltage of 2.23 V respectively at a relative working orientation of 50° . Meanwhile, due to the in-plane symmetry, the output current and output voltage at 40° were very close to those at 50° . Although the output current and output voltage decreased slightly as θ increases as a result of the decrease of the effective friction area caused by the

mismatched gratings between the upper part and the lower part of the 2DW-WTNG, these experimental results strongly validated that the 2DW-WTNG could work normally at different working orientations. Benefited from the cylindrical composite fiber, its smooth surface made the sliding become continuously and re-posablely, rather than the wobbling sliding in the narrow gratings with obviously raised edge made by lithographic process. Similarly, if an external motion along arbitrary in-plane direction was applied on the upper part of the 2DW-WTNG, it slid along the motion direction and rubbed with the lower part, and thus, the motion energy could be harvested and converted into electricity.

As an energy harvester, the output of the 2DW-WTNG should be high enough for powering some electronic devices. As shown in Fig. 5a, the 2DW-WTNG was connected with a bridge rectifier and then connected with two branch circuits. With the bridge rectifier, the AC output of the 2DW-WTNG was transformed into direct current (DC) output. The rectified DC signal is shown in Fig. 5b. When connecting the bridge rectifier to the first branch circuit, the rectified DC signal was directly used to light up the red LED as shown in the inset and in Additional file 1: Video S1. When the bridge rectifier was connected to the second branch circuit, the electricity from the 2DW-WTNG

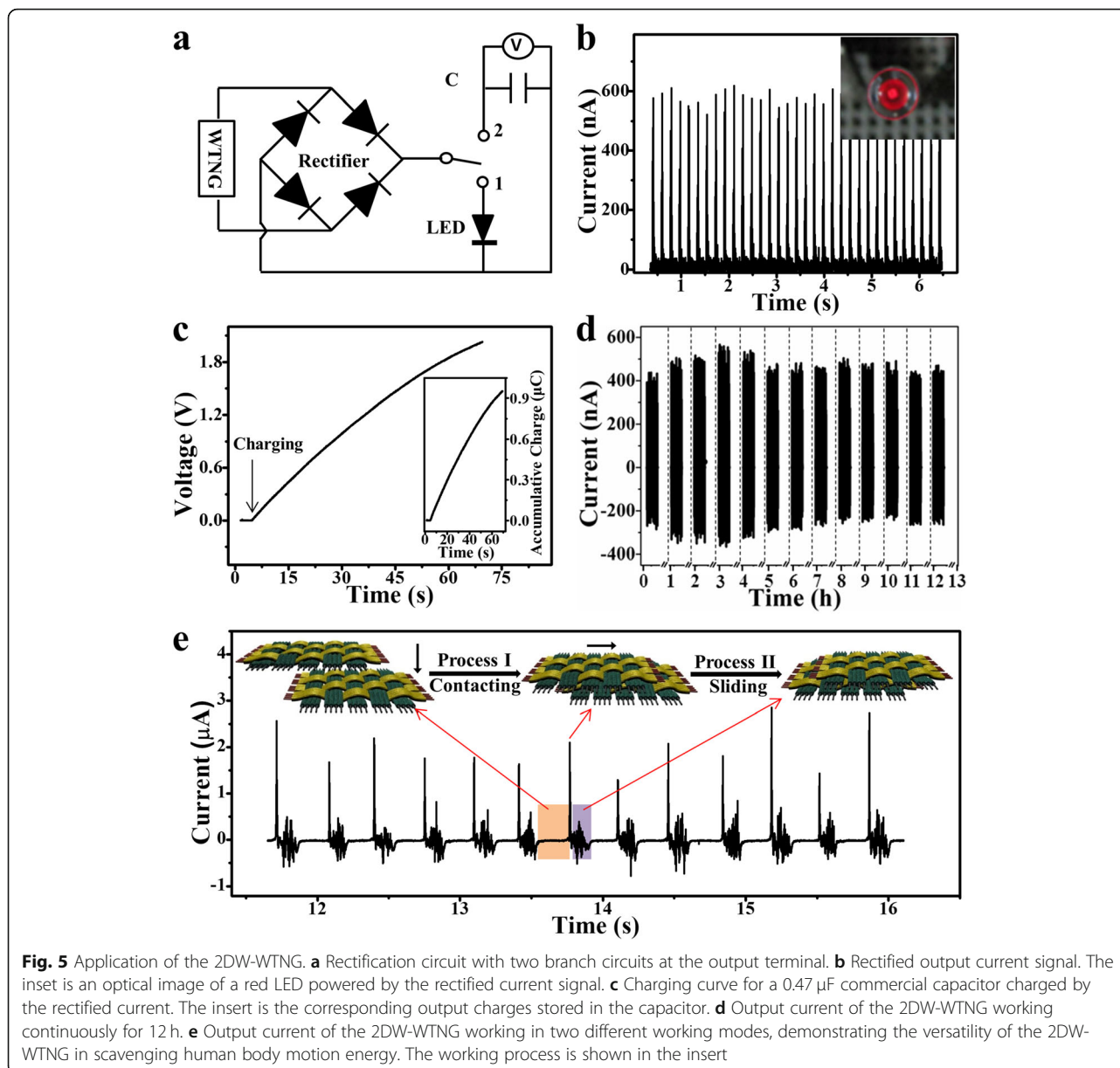


charged a $0.47 \mu\text{F}$ commercial capacitor. The charging curve is shown in Fig. 5c and its corresponding charge amount stored in the capacitor is shown in the inset. The capacitor was charged to 1.84 V in 1 min, and the corresponding charge density reached 3.84 mC/m^2 . These two tests indicated that as an energy harvester, the 2DW-WTNG could not only be used as a convenient emergency power supply, but it could also fuel energy into a storage cell. Furthermore, the stability of the 2DW-WTNG is an essential factor to ensure its practical applications. Here, the 2DW-WTNG's stability was tested by making it continuously works for 12 h at a sliding speed of 0.1 m/s and a sliding displacement of 8 mm . The current curves in 10 s for every hour are shown in Fig. 5d, and little change can be found in the output current value after 12-h continuous work, exhibiting highly stable power generation performance. Additionally, to demonstrate the versatility of the 2DW-WTNG in scavenging energy in various types, a group of electrical measurements was conducted on the 2DW-WTNG. As shown in the inset in Fig. 5e, the effective friction occurs as the upper part of the 2DW-WTNG firstly vertically contacted with the lower part of the 2DW-WTNG (process I), and then horizontally slid on the lower 2DW-WTNG (process II). During the measurement, the contacting-sliding-separating operation was repeated for several times, and its output current is shown in Fig. 5e. For the first vertically contacting

friction process, there was a high but narrow output peak, and then for the following horizontally sliding friction process, there was a low but wide peak. At the last vertically separating process for next measuring cycle, a high but narrow output peak should appear but was missing. This can be attributed to two reasons. One is that the upper part of the 2DW-WTNG has slid out the opposite lower part of the 2DW-WTNG, and the electric potential was almost balanced. The other one is that the last vertically separating process was rather slow, so the electric potential quickly reached equilibrium in the air. The synthetical analysis confirmed that these two kinds of output current peaks were consistent with the characteristics of 2DW-WTNG's two working modes, displaying its strong adaptability to scavenge energy from vertical positive pressure and horizontal tangential force in human body motions.

Conclusions

In summary, a new WTNG with 2D woven structure as a wearable power source was developed through an easily scalable approach. This 2DW-WTNG has demonstrated its good capability of converting the mechanical energy into electricity and generated a current density up to 2.73 mA/m^2 . It could instantaneously power a commercial red LED without the need for an energy storage process. It can also be used to charge a $0.47 \mu\text{F}$ capacitor to 1.84 V in 1 min and the charge density



reached 3.84 mC/m^2 in 1 min. Benefited from the robustness of the core-shell structured fiber and the woven structure, the 2DW-WTNG could work in arbitrary sliding directions. Furthermore, the 2DW-WTNG was applied to harvest mechanical energy with different forms and worked continuously for 12 h with steady output. The remarkable performance, flexibility, maneuverability, and robustness enabled the 2DW-WTNG to harvest the mechanical energy from human body motion and to power low-power electronic products. Most importantly, this work provides a designed model for massive production of fiber-based wearable generator, which will greatly promote the development of personal electronic devices.

Additional file

Additional file 1: **Video S1**. Video of instantly lighting a red LED. (AVI 1334 kb)

Abbreviations

2DW-WTNG: 2D woven wearable triboelectric nanogenerator; AC: Alternating current; DC: Direct current; LED: Light-emitting diode; SEM: Scanning electron microscope; WTNG: Wearable triboelectric nanogenerator

Acknowledgements

We sincerely appreciate the support from NSFC (NO. 51472111, No. 81801847), the Fundamental Research Funds for the Central Universities (Grant No. JB191407), the Fundamental Research Funds for the Central Universities (No. lzujbky-2018-ot04), and the National Program for Support of Top-notch Young Professionals.

Authors' Contributions

YQ conceived the experiment. JL and LG performed the experiments. JL and NC analyzed the experimental data. SB plotted the structure diagram of the 2DW-WTNG. SL and QX checked the data. JL and LG wrote the manuscript. RY and FZ co-wrote the manuscript. All authors read and approved the final manuscript.

Availability of Data and Materials

The data and the analysis in the current work are available from the corresponding authors on reasonable request.

Competing Interests

The authors declare that they have no competing interests.

Author details

¹Institute of Nanoscience and Nanotechnology, Lanzhou University, Lanzhou 730000, China. ²School of Advanced Materials and Nanotechnology, Xidian University, Xi'an 710071, China. ³State Key Laboratory of Solid Lubrication, Lanzhou Institute of Chemical Physics, Chinese Academy of Sciences, Lanzhou 730000, China.

Received: 15 May 2019 Accepted: 30 August 2019

Published online: 11 September 2019

References

- Marculescu D, Marculescu R, Zamora NH, Stanley MP, Khosla PK, Park S, Jayaraman S, Jung S, Lauterbach C, Weber W, Kirstein T, Cottet D, Grzyb J, Troster G, Jones M, Martin T, Nakad Z (2003) Electronic textiles: a platform for pervasive computing. *Proc IEEE* 91:1995–2018
- Forrest SR (2004) The path to ubiquitous and low-cost organic electronic appliances on plastic. *Nature* 428:911–918
- Sahin O, Kayacan O, Bulgun EY (2005) Smart textiles for soldier of the future. *Def Sci J* 55:195–205
- Kim DH, Kim YS, Wu J, Liu ZJ, Song JZ, Kim HS, Huang YY, Hwang KC, Rogers JA (2009) Ultrathin silicon circuits with strain-isolation layers and mesh layouts for high-performance electronics on fabric, vinyl, leather, and paper. *Adv Mater* 21:3703–3707
- Klauk H (2010) Organic thin-film transistors. *Chem. Soc. Rev.* 39:2643–2666
- Danto S, Ruff Z, Wang Z, Joannopoulos JD, Fink Y (2011) Ovonic memory switching in multimaterial fibers. *Adv Funct Mater* 21:1095–1011
- Park M, Im J, Shin M, Min Y, Park J, Cho H, Park S, Shim M, Jeon S, Chung DY, Bae J, Park J, Jeong U, Kim K (2012) Highly stretchable electric circuits from a composite material of silver nanoparticles and elastomeric fibres. *Nat Nanotechnol* 7:803–809
- Wang C, Hwang D, Yu Z, Takei K, Park J, Chen T, Ma B, Javey A (2013) User-interactive electronic skin for instantaneous pressure visualization. *Nat Mater* 12:899–904
- Jang KI, Han SY, Xu S, Mathewson KE, Zhang Y, Jeong JW, Kim GT, Webb RC, Lee JW, Dawidczyk TJ, Kim RH, Song YM, Yeo WH, Kim S, Cheng H, Rhee S, Chung J, Kim B, Chung HU, Lee D, Yang Y, Cho M, Gaspar JG, Carbonari R, Fabiani M, Gratton G, Huan Y, Rogers JA (2014) Rugged and breathable forms of stretchable electronics with adherent composite substrates for transcutaneous monitoring. *Nat Commun* 5:4779
- Tee BC-K, Chortos A, Berndt A, Nguyen AK, Tom A, McGuire A, Lin ZC, Tien K, Bae WG, Wang H, Mei P, Chou H-H, Cui B, Deisseroth K, Ng TN, Bao Z (2015) A skin-inspired organic digital mechanoreceptor. *Science* 350:313–316
- Gao W, Emaminejad S, Nyein HY, Challa S, Chen K, Peck A, Fahad HM, Ota H, Shiraki H, Kiriya D, Lien D-H, Brooks GA, Davis RW, Javey A (2016) Fully integrated wearable sensor arrays for multiplexed in situ perspiration analysis. *Nature* 529:509–514
- Gaikwad AM, Whiting GL, Steingart DA, Arias AC (2011) Highly flexible, printed alkaline batteries based on mesh-embedded electrodes. *Adv Mater* 23:3251
- Pu X, Yang G, Yu C (2004) Liquid-type cathode enabled by 3D sponge-like carbon nanotubes for high energy density and long cycling life of Li-S batteries. *Adv Mater* 26:7456
- Zhou G, Li F, Cheng H-M (2014) Progress in flexible lithium batteries and future prospects. *Energy Environ Sci* 7:1307
- Xu S, Zhang YH, Cho J, Lee J, Huang X, Jia L, Fan JA, Su JY, Su J, Zhang HG, Cheng HY, Lu BW, Yu CJ, Chuang C, Kim TI, Song T, Shigetani K, Kang S, Dagdeviren CN, Petrov I, Braun PV, Huang YG, Paik U, Rogers JA (2013) Stretchable batteries with self-similar serpentine interconnects and integrated wireless recharging systems. *Nat Commun* 4:1543
- Son D, Lee J, Qiao ST, Ghaffari R, Kim J, Lee JE, Song CY, Kim SJ, Lee DJ, Jun SW, Yang SX, Park M, Shin J, Do K, Lee M, Kang K (2014) Multifunctional wearable devices for diagnosis and therapy of movement disorders. *Nat Nanotechnol* 9:397–404
- Xu S, Zhang YH, Jia L, Mathewson KE, Jang K-I, Kim J, Fu HR, Huang X, Chava P, Wang RH, Bhole S, Wang LZ, Na YJ, Guan Y, Flavin M, Han ZS, Huang YG, Rogers JA (2014) Soft microfluidic assemblies of sensors, circuits, and radios for the skin. *Science* 344:70–74
- Park SI, Brenner DS, Shin G, Morgan CD, Copits BA, Chung HU, Pullen MY, Noh KN, Davidson S, Oh SJ, Yoon J, Jang KI, Samineni VK, Norman M, Grajales-Reyes JG, Vogt SK, Sundaram SS, Wilson KM, Ha JS, Xu R (2015) Soft, stretchable, fully implantable miniaturized optoelectronic systems for wireless optogenetics. *Nat Biotechnol* 33:1280–1286
- Weng W, Chen P, He S, Sun X, Peng H (2016) Smart electronic textiles. *Angew Chem Int Ed* 55:6140–6169
- Qi Y, McAlpine MC (2010) Nanotechnology-enabled flexible and biocompatible energy harvesting. *Energy Environ Sci* 3:1275–1285
- Fan FR, Lin L, Zhu G, Wu W, Zhang R, Wang ZL (2012) Transparent triboelectric nanogenerators and self-powered pressure sensors based on micropatterned plastic films. *Nano Lett* 12:3109–3114
- Nguyen V, Yang RS (2013) Effect of humidity and pressure on the triboelectric nanogenerator. *Nano Energy* 2:604–608
- Wang ZL (2014) Triboelectric nanogenerators as new energy technology and self-powered sensors - principles, problems and perspectives. *Faraday Discuss* 176:447–458
- Liu JM, Cui NY, Gu L, Chen XB, Bai S, Zheng YB, Hu CX, Qin Y (2016) A three-dimensional integrated nanogenerator for effectively harvesting sound energy from the environment. *Nanoscale* 8:4938–4944
- Kirkwood JG, Westheimer FH (1938) The electrostatic influence of substituents on the dissociation constants of organic acids. *J Chem Phys* 6:513–517
- Pitzer KS (1975) Thermodynamics of electrolytes. V. effects of higher-order electrostatic terms. *J Solut Chem* 4:249–265
- Feller SE, Pastor RW, Rojnuckarin A, Bogusz S (1996) Effect of electrostatic force truncation on interfacial and transport properties of water. *J Phys Chem* 100:17011–17020
- Castle GSP (1997) Contact charging between insulators. *J Electrostat* 40:13–20
- McCarty LS, Whitesides GM (2008) Electrostatic charging due to separation of ions at interfaces: contact electrification of ionic electrets. *Angew Chem Int Ed* 47:2188–2207
- Baytekin HT, Patashinski AZ, Branicki M, Baytekin B, Soh S, Grzybowski BA (2011) The mosaic of surface charge in contact electrification. *Science* 333:308–312
- Zhang HL, Yang Y, Hou T-CH, Su YJ, Hu CG, Wang ZL (2013) Triboelectric nanogenerator built inside clothes for self-powered glucose biosensors. *Nano Energy* 2:1019
- Zhong JW, Zhang Y, Zhong QZ, Hu QY, Hu B, Wang ZL, Zhou J (2014) Fiber-based generator for wearable electronics and mobile medication. *ACS Nano* 8:6273–6280
- Kim KN, Chun J, Kim JW, Lee KY, Park JU, Kim SW (2015) Highly stretchable 2D fabrics for wearable triboelectric nanogenerator under harsh environments. *ACS Nano* 9:6394–6400
- Pu X, Li LX, Song HQ, Du CH, Zhao ZF, Jiang CY, Cao GZ, Hu WG, Wang ZL (2015) A self-charging power unit by integration of a textile triboelectric nanogenerator and a flexible lithium-ion battery for wearable electronics. *Adv Mater* 27:2472–2478
- Chen J, Huang Y, Zhang NN, Zou HY, Liu RY, Tao CY, Fan X, Wang ZL (2016) Micro-cable structured textile for simultaneously harvesting solar and mechanical energy. *Nat Energy* 1:16138
- Yi F, Yang J, Wang XF, Niu SM, Li SM, Liao QL, Xu YL, You Z, Zhang Y, Wang ZL (2016) Stretchable and waterproof self-charging power system for harvesting energy from diverse deformation and powering wearable electronics. *ACS Nano* 10:6519
- Lai YC, Deng JN, Niu SM, Peng WB, Wu CS, Liu RY, Wen Z, Wang ZL (2016) Electric eel-skin-inspired mechanically durable and super-stretchable nanogenerator for deformable power source and fully autonomous conformable electronic-skin applications. *Adv Mater* 28:10024
- Wang J, Li SM, Yi F, Zi YL, Lin J, Wang XF, Xu YL, Wang ZL (2016) Sustainably powering wearable electronics solely by biomechanical energy. *Nat Commun* 7:12744

39. Wen Z, Yeh MH, Guo HY, Wang J, Zi YL, Xu WD, Deng JN, Zhu L, Wang X, Hu CG, Zhu LP, Sun XH, Wang ZL (2016) Self-powered textile for wearable electronics by hybridizing fiber-shaped nanogenerators, solar cells, and supercapacitors. *Science Advances* 2:1600097
40. Chen SW, Cao X, Wang N, Ma L, Zhu HR, Willander M, Jie Y, Wang ZL (2016) Triboelectric nanogenerator for sustainable wastewater treatment via a self-powered electrochemical process. *Adv Energy Mater* 7:1601255
41. Zhang Q, Liang QJ, Liao QL, Yi F, Zheng X, Ma MY, Gao FF, Zhang Y (2017) Service behavior of multifunctional triboelectric nanogenerators. *Adv Mater* 29:1606703
42. Zhang SL, Lai YC, He X, Liu RY, Zi YL, Wang ZL (2017) Auxetic foam-based contact-mode triboelectric nanogenerator with highly sensitive self-powered strain sensing capabilities to monitor human body movement. *Adv Funct Mater* 27:1606695
43. Zhang Q, Liang QJ, Liao QL, Ma MY, Gao FF, Zhao X, Song YD, Song LJ, Xun XC, Zhang Y (2018) An amphiphobic hydraulic triboelectric nanogenerator for a self-cleaning and self-charging power system. *Adv Funct Mater* 28:1803117
44. Zhang Q, Liang QJ, Zhang Z, Kang Z, Liao QL, Ding Y, Ma MY, Gao FF, Zhao X, Zhang Y (2018) Electromagnetic shielding hybrid nanogenerator for health monitoring and protection. *Adv Funct Mater* 28:1703801
45. Kim S, Gupta MK, Lee KY, Sohn A, Kim TY, Shin KS, Kim D, Kim SK, Lee KH, Shin HJ, Kim DW, Kim SW Transparent flexible graphene triboelectric nanogenerators. *Adv Mater* 26:3918
46. Li XH, Lin ZH, Cheng G, Wen XN, Liu Y, Niu SM, Wang ZL (2014) 3D fiber-based hybrid nanogenerator for energy harvesting and as a self-powered pressure sensor. *ACS Nano* 8:10674
47. Zhang Q, Zhang Z, Liang QJ, Gao FF, Yi F, Ma MY, Liao QL, Kang Z, Zhang Y (2019) Green hybrid power system based on triboelectric nanogenerator for wearable/portable electronics. *Nano Energy* 55:151
48. Jung S, Lee J, Hyeon T, Lee M, Kim DH (2014) Fabric-based integrated energy devices for wearable activity monitors. *Adv Mater* 26:6329–6334
49. Seung W, Gupta MK, Lee KY, Shin KS, Lee JH, Kim TY, Kim S, Lin JJ, Kim JH, Kim SW (2015) Nanopatterned textile-based wearable triboelectric nanogenerator. *ACS Nano* 9:3501–3509
50. Cui NY, Liu JM, Gu L, Bai S, Chen XB, Qin Y (2015) Wearable triboelectric generator for powering the portable electronic devices. *ACS Appl Mater Interfaces* 7:18225–18230
51. Pu X, Song WX, Liu MM, Jiang CY, Du CH, Jiang CY, Huang X, Zou DC, Hu WG, Wang ZL (2016) Wearable power-textiles by integrating fabric triboelectric nanogenerators and fiber-shaped dye-sensitized solar cells. *Adv Energy Mater*:1601048
52. Pu X, Li LX, Liu MM, Jiang CY, Du CH, Zhao ZF, Hu WG, Wang ZL (2016) Wearable self-charging power textile based on flexible yarn supercapacitors and fabric nanogenerators. *Adv Mater* 28:98–105
53. He X, Zi YL, Guo HY, Zheng HW, Xi Y, Wu CS, Wang J, Zhang W, Lu CH, Wang ZL (2017) A highly stretchable fiber-based triboelectric nanogenerator for self-powered wearable electronics. *Adv Funct Mater* 27:1604378
54. Zhou T, Zhang C, Han CB, Fan FR, Tang W, Wang ZL (2014) Woven structured triboelectric nanogenerator for wearable devices. *ACS Appl Mater Interfaces* 6:14695–14701
55. Lai YC, Deng JN, Zhang SL, Niu SM, Guo H, Wang ZL (2016) Extraordinarily sensitive and low-voltage operational cloth-based electronic skin for wearable sensing and multifunctional integration uses: a tactile-induced insulating-to-conducting transition. *Adv Funct Mater* 27:1604462
56. Dong K, Wang YC, Deng JN, Dai YJ, Zhang SL, Zou HY, Gu BH, Sun BZ, Wang ZL (2017) A highly stretchable and washable all-yarn-based self-charging knitting power textile composed of fiber triboelectric nanogenerators and supercapacitors. *ACS Nano* 11:9490–9499
57. Dong K, Deng JN, Zi YL, Wang Y-CH, Xu CH, Zou HY, Ding WB, Dai YJ, Gu BH, Sun BZ, Wang ZL (2017) 3D orthogonal woven triboelectric nanogenerator for effective biomechanical energy harvesting and as self-powered active motion sensors. *Adv Mater* 29:1702648

Publisher's Note

Springer Nature remains neutral with regard to jurisdictional claims in published maps and institutional affiliations.

Submit your manuscript to a SpringerOpen[®] journal and benefit from:

- Convenient online submission
- Rigorous peer review
- Open access: articles freely available online
- High visibility within the field
- Retaining the copyright to your article

Submit your next manuscript at ► [springeropen.com](https://www.springeropen.com)
